One-Dimensional Cd^{II} Coordination Polymers: Solid Solutions with Ni^{II}, Thermal Stabilities and Structures

Dejana Vujovic,*[a] Helgard G. Raubenheimer,[a] and Luigi R. Nassimbeni[b]

Keywords: Coordination polymers / Solid solutions / Cadmium complexes

Reactions of $Cd(NCS)_2$ with 2-, 3- and 4-aminobenzonitrile ligands (2ABN, 3ABN and 4ABN respectively) have produced one-dimensional chain polymers of the general formula $[M(NCS)_2(ABN)_2]_n$ with the metal centres linked by double NCS^- bridges. The three cadmium polymers $[Cd(NCS)_2(3ABN)_2]_n$ (**1**), $[Cd(NCS)_2(2ABN)_2]_n$ (**2**) and $[Cd(NCS)_2(4ABN)_2]_n$ (**3**) all differ in their hydrogen-bonding patterns. In terms of ABN coordination, both **1** and **2** exhibit terminal amine coordination while in **3** the ABNs are coordinated through the cyano groups. Crystalline solid solutions of **1** of general formula $[Cd_{1-x}Ni_x(NCS)_2(3ABN)_2]_n$, containing nickel and cadmium in varying proportions, have also been prepared in order to establish the influence of the metal ratio on the thermal stability and bonding parameters of the polymers. The coordination polymers are not good candidates for forming clathrates while their thermal stability (ranging between 147 and 244 °C) depends on the position of functional groups on the ABN ligands and on the Cd:Ni ratio in the solid solutions. The new polymers have been characterised by single crystal X-ray diffraction, X-ray powder diffraction, electron microscopy, infrared spectroscopy, thermogravimetry and differential scanning calorimetry.

Introduction

Self-assembled coordination polymers have attracted considerable recent interest due to both their many interesting architectures[1−6] and numerous applications.[7−9] Such systems are often tunable by making subtle changes to the reaction conditions, such as the choice of counterion and solution pH, that allow the deliberate design of compounds with luminescent,[10] superconducting[11,12] or magnetic properties[13,14] and also compounds that can be used as nanofibres,[15] in catalysis,[16] in separation processes,[17,18] for gas and liquid storage[19] and in nonlinear optics.[20,21]

We have prepared previously one-dimensional coordination polymers of Ni^{II} with aminobenzonitrile isomers and thiocyanate ions as ligands.[22] The structural features and thermal stability of the polymers were determined by the position of the functional groups on the ABN isomers as well as the introduction of guest molecules into the structures. Furthermore, the ABN isomers not only afford hydrogen-bonded networks, but also lead to the possible formation of 1-, 2- and 3-dimensional polymer networks due to different coordination preferences such as coordination to the metal centre in monodentate (albeit ambidentately using either amine or cyanide nitrogens), bidentate (2ABN) or in a bridging fashion (using both nitrogen donors).

Most studied coordination polymers are unimetallic. Addition of a second metal to inorganic compounds is a well-established procedure in industry to modify and improve material properties. Studies on bimetallic coordination polymers usually involve either two different metals in different[23] or similar[24] oxidation states or the same metal in two different oxidation states.[25] The resultant new structure usually differs significantly from the starting one, with the two metals located in different positions along the polymeric chain. Coordination compounds with both metals at the same site of an unchanged structure have also been investigated; this work also concentrates on such bimetallic compounds. Magnetic phase transition studies are an example of this type of work. They involve Hofmann-type clathrates of the general formula $M(NH_3)_2M'(CN)_4{\cdot}2G$ (where M and M′ are transition metals), the magnetic properties of which are affected by diluting one of the metal sites with another metal located at the same position in the overall structure.[26−29]

Extensive studies have been carried out over the past three decades on coordination compounds of SCN^- using various transition metals. Most early work again involved Hofmann-type compounds, which, over the years, has expanded to include the design of materials and architectures with specific properties. SCN^- is a highly versatile ligand with both terminal and bridging coordination possibilities. As a terminal ligand it is either *S*- or *N*-coordinated, while as a bridging ligand it is most often coordinated in a bidentate or tridentate fashion (however, 13 possible bonding

[a] Department of Chemistry, University of Stellenbosch, Private Bag X1, Matieland 7602, South Africa
[b] Department of Chemistry, University of Cape Town, Rondebosch 7701, South Africa

modes have been identified).[30] The result is a wide variety of possible complexes, clusters and polymers (1-D single, double and triple bridged chains and 2-D and 3-D networks).[31,32]

Here, as part of a continuing study, we report on the structural and thermal influence of a metal on coordination polymers. This has been achieved by (i) changing the metal centre from Ni^{II} to Cd^{II} and/or (ii) introducing both metals in different ratios into the starting mixtures. Changing the metal centre from Ni^{II} to Cd^{II} afforded dramatically different polymeric structures **2** and **3** with 2ABN and 4ABN ligands in the presence of thiocyanate. Conversely, when $Cd(NCS)_2$ is treated with 3ABN the resultant polymer **1** is isostructural with its nickel counterpart, giving the option of introducing both metals in different proportions into such structures. Crystal structures, thermodynamic stabilities and metal concentrations in structures of the general formula $[Cd_{1-x}Ni_x(NCS)_2(3ABN)_2]_n$ have been determined by experimental methods (**4**−**7**).

Results and Discussion

Crystal Structure Analysis

Crystalline samples of the cadmium polymers were prepared by slow evaporation of mixtures of ethanolic ABN and $Cd(NCS)_2$ solutions. The crystals grew over a period of 1−3 days. Salient crystal and experimental data (Table 1) and hydrogen-bonding details (Table 2) are summarised here.

Crystal structure analysis revealed that **1** is isostructural with its previously reported nickel analogue **8**.[22] One-dimensional, double-stranded chain polymers were formed with a metal-to-3ABN ratio of 1:2. Thiocyanate double bridges propagate the chain along the crystallographic *b*-axis with the amine-bonded 3ABN ligands at axial positions. Adjacent polymer units are hydrogen-bonded through their amine and nitrile moieties, producing sheets parallel to the (011) plane. The structure of the coordination polymer **1** is shown in Figure 1.

Table 2. Hydrogen-bond lengths and angles

	Donor (D)	Acceptor (A)	D−H (Å)	D···A (Å)	D−H···A (°)
1	N(7A)	N(9A)#[1]	0.87(1)	3.159(3)	174(2)
2	N(7B)	N(9B)#[2]	0.90	3.14(3)	154
	N(7A)	N(9A)#[3]	0.90	3.16(2)	146
	N(7A)	N(9A)#[4]	0.90	3.126(17)	167
3	N(7A)	S1#[5]	0.92(3)	3.569(4)	157(4)
4	N(7A)	N(9A)#[6]	0.90(2)	3.149(3)	174(3)
5	N(7A)	N(9A)#[7]	0.88(2)	3.152(2)	169(2)
6	N(7A)	N(9A)#[8]	0.90(2)	3.150(3)	172(3)
7	N(7A)	N(9A)#[9]	0.88(1)	3.144(1)	169(1)
8[22]	N(7A)	N(9A)#[6]	0.82(1)	3.125(2)	171(2)

#1: $-x+1, y+1, -z+1/2$; #2: $x+1, y, z$; #3: $-x+1, -y-1, -z$; #4: $x-1, y, z$; #5: $x+1/2, -y-1/2, z+1/2$. #6: $-x, y+1, -z+3/2$; #7: $-x+1, y-1, -z+3/2$; #8: $-x, y-1, -z+1/2$; #9: $-x+1, y+1, -z+3/2$.

Polymers **2** and **3** are also one-dimensional chain structures with double thiocyanate bridges. 2ABN ligands in **2** are coordinated to the metal through the amine nitrogens and are disordered over two positions (Figure 2) while 4ABN molecules in **3** are coordinated to the cadmium centres through the cyanide nitrogens (Figure 3). The disordered 2ABN molecules have site occupancies of 50% for each of the two disordered positions, A and B, with the whole structure stabilised by inter- and intramolecular hydrogen bonding. When 2ABN are in position A, each amine group is hydrogen-bonded to two adjacent cyanide ni-

Table 1. Crystallographic data

Compound	**1**	**2**	**3**	**4**	**5**	**6**	**7**	**8**[22]
Empirical formula	$CdC_{16}H_{12}N_6S_2$	$CdC_{16}H_{12}N_6S_2$	$CdC_{16}H_{12}N_6S_2$	$Cd_{0.70}Ni_{0.30}C_{16}H_{12}N_6S_2$	$Cd_{0.59}Ni_{0.41}C_{16}H_{12}N_6S_2$	$Cd_{0.51}Ni_{0.49}C_{16}H_{12}N_6S_2$	$Cd_{0.23}Ni_{0.77}C_{16}H_{12}N_6S_2$	$NiC_{16}H_{12}N_6S_2$
Molecular mass	464.84	464.84	464.84	448.73	442.82	438.53	423.49	411.15
T (K)	173(2)	173(2)	173(2)	173(2)	173(2)	173(2)	173(2)	173(2)
Crystal system	monoclinic	triclinic	monoclinic	monoclinic	monoclinic	monoclinic	monoclinic	monoclinic
Space group	*C*2/*c*	$P\bar{1}$	$P2_1/n$	*C*2/*c*	*C*2/*c*	*C*2/*c*	*C*2/*c*	*C*2/*c*
a (Å)	17.1917(3)	5.9978(3)	7.5212(4)	17.1187(5)	17.0903(3)	17.0787(3)	17.0122(3)	16.9554(3)
b (Å)	5.6604(1)	7.3826(1)	5.7460(3)	5.6369(1)	5.6208(1)	5.6204(1)	5.5829(1)	5.5542(1)
c (Å)	18.5651(3)	9.9158(3)	20.6145(12)	18.4892(5)	18.4630(4)	18.4439(4)	18.3755(4)	18.2897(3)
α (°)	90	88.927(2)	90	90	90	90	90	90
β (°)	92.428(1)	84.145(2)	93.284(3)	92.445(1)	92.426(1)	92.453(1)	92.485(1)	92.491(1)
γ (°)	90	78.552(3)	90	90	90	90	90	90
V (Å^3)	1805.0(1)	428.1(1)	889.4(1)	1782.5(1)	1772.0(1)	1768.8(1)	1743.6(1)	1720.8(1)
Z	4	1	2	4	4	4	4	4
$D_{calcd.}$ (Mg·m^{-3})	1.711	1.803	1.736	1.672	1.660	1.645	1.613	1.587
μ (mm^{-1})	1.452	1.531	1.474	1.429	1.423	1.413	1.396	1.381
F(000)	920	230	460	896	887	881	858	840
Refl. collected	4076	3700	3916	3362	3585	3939	3785	5462
Unique reflections	2145	1958	2176	1801	1926	2101	1992	2120
R_{int}	0.019	0.019	0.021	0.021	0.017	0.012	0.011	0.018
Data/restraints/parameters	2145/2/123	1958/2/197	2176/2/123	1801/2/130	1926/2/129	2101/2/129	1992/2/129	2120/0/123
R [$I > 2\sigma(I)$]	0.0232	0.0248	0.0376	0.0281	0.0224	0.0204	0.0199	0.0226
R (all data)	0.0346	0.0280	0.0508	0.0433	0.0307	0.0256	0.0238	0.0254
wR' [$I > 2\sigma(I)$]	0.0499	0.0476	0.0789	0.0543	0.0550	0.0440	0.0478	0.0587
wR' (all data)	0.0528	0.0484	0.0848	0.0585	0.0580	0.0461	0.0492	0.0602

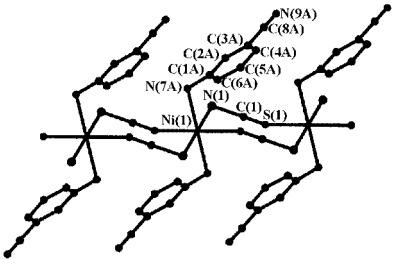

Figure 1. Section of the molecular structure of polymer **1**, showing the numbering scheme (the same numbering scheme was used for all compounds)

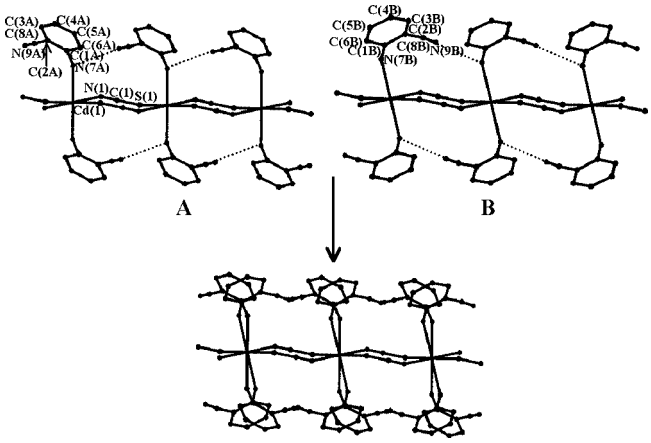

Figure 2. Section of the molecular structure of polymer **2**, showing disorder, hydrogen bonding and the numbering scheme

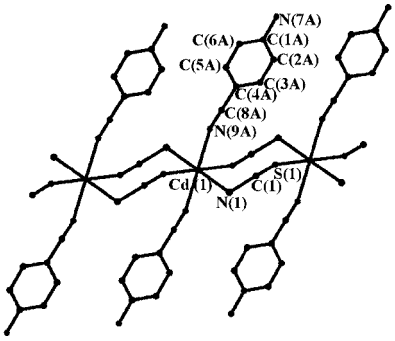

Figure 3. Section of the molecular structure of polymer **3**, showing the numbering scheme

trogens − one on the adjacent monomer unit of the same polymer strand and the other on a symmetry related strand. Intermolecular hydrogen bonding gives rise to the sheets parallel to the (110) plane. Position B only leads to intramolecular hydrogen-bonding. For **3**, only weak hydrogen bonds are present between the amine groups of one polymer strand and the thiocyanate sulfur atoms of another.

The introduction of several compounds (benzene, ABN, chloroform, toluene, naphthalene and linear and aromatic alcohols) into the respective starting mixtures afforded the polymers **1**−**6** (except for **7**) but gave no inclusion compounds. Thus, the cadmium-polymer formation is unaffected by potential guest molecules in the crystallisation medium. The only exception occurs for compound **7** when benzene is used as a guest and the nickel content in the mixed metal exceeds 75%. Here, two products are formed: the original Cd polymer **1** and the previously reported[22] nickel inclusion compound $[Ni(NCS)_2(3ABN)_2]_n$·(benzene). Interestingly, by changing the metal centre, we can suppress or activate the inclusion capability of a polymer. In addition, the introduction of a guest species in nickel polymers resulted in a structural change, due to differences in the modes of ligand coordination around the metal centre,[22] while the same was not observed with cadmium.

These results indicate different behaviours of cadmium and nickel in saturated solutions: nickel polymers can be tuned in terms of both their polymer structure and the formation of cavities, due to inclusion, while such a process is not useful for cadmium-containing compounds.

Solid solutions **4**−**7** were prepared as described in the Exp. Sect. The crystals are green, the colour intensity increasing with increasing concentration of nickel. Relatively large crystals of these bimetallic polymers were selected and then cut in two: one part for single-crystal X-ray analysis and the other for electron microscopy. This is important in avoiding ambiguous results as the ratio of each metal in the crystal could vary from batch to batch and also within the same batch. Crystals chosen for analysis were approximately 2.2 × 1.4 × 0.5 mm before cutting. The Cd:Ni ratio, determined at four sites for each crystal by electron microscopy, was reasonably homogeneous (Figure 4).

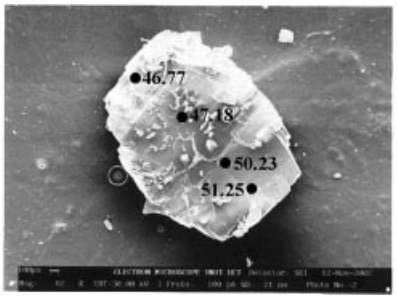

Figure 4. Electron microscopy image of a crystal of polymer **4**, showing the location and the results of measurements (as % Cd)

All four bimetallic compounds **4**−**7** are isostructural with the parent cadmium (**1**) and nickel (**8**) polymers, with the two metals occupying the same site. Structures were solved and refined by first locating all non-hydrogen atoms, then refining them anisotropically, and adding all the hydrogens to the final model. The relative metal composition in the structure was determined as the final part of refinement. The metal site was treated as being disordered as it may be occupied by a different metal atom in different unit cells. We attempted several different methods outlined in the literature:[33] (i) site occupancy values were allowed to refine while the displacement parameters remained fixed, having the same value; (ii) site occupancy values and the displacement parameters were refined simultaneously; (iii) once the site occupancy values were refined according to (i) the displacement parameters were also allowed to refine. All three

methods were unsuccessful in refining the four structures and, therefore, the following procedure was adopted: Site occupancies of the Ni and Cd atoms were systematically changed from 0 to 1 in 5% increments and the isotropic parameters were not constrained but instead allowed to refine. When these were in the range $0.01 < U_{iso} < 0.03$, the site occupancies were analysed in 1% increments. This technique allowed a final refinement in which the metal atoms had unconstrained anisotropic thermal parameters.

The Cd:Ni ratios determined by crystal structure refinement and electron microscopy are in very good agreement (Figure 5).

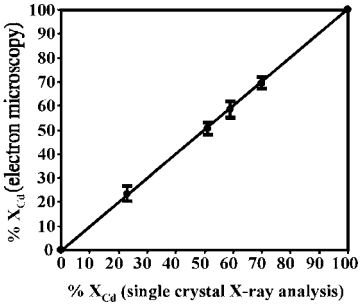

Figure 5. Percentage mol fraction cadmium, X_{Cd}, determined by electron microscopy and by single crystal X-ray diffraction refinement

For two isostructural parent compounds, where one ion is substituted by another at some sites, previous studies of inorganic solid solutions indicate that ions that can substitute one another[34] should not differ in size by more than 10−15%, so as to prevent drastic lattice distortions or changes in packing. These lattice distortions were not observed in our study even though the radii[35] of Cd^{2+} and Ni^{2+} are 0.95 and 0.69 Å, respectively, corresponding to a 38% difference in size. This could be because the volume occupied by the two metal atoms in the unit cell is relatively small compared with that of all the other atoms (in thiocyanate and 3ABN ligands).

Table 3. Selected bond lengths and angles

	Bond lengths (Å)			Bond angles (°)
	M−NCS	M−SCN	M−NH_2	N−M−S
1	2.293(1)	2.709(2)	2.389(2)	93.91(4)
2	2.313(1)	2.719(5)	2.391(5)[a] 2.445(6)[b]	91.03(4)
3	2.290(3)	2.722(1)	[c]	90.92(9)
4	2.215(3)	2.662(1)	2.320(2)	93.69(6)
5	2.158(4)	2.633(1)	2.273(3)	93.35(4)
6	2.159(2)	2.631(1)	2.272(2)	93.37(4)
7	2.065(1)	2.577(1)	2.188(1)	93.08(3)
8[22]	2.016(1)	2.544(1)	2.137(1)	92.98(3)

[a] Ring A. [b] Ring B. [c] Cd−NC = 2.341(3) Å.

Table 3 shows selected bond lengths and angles involving the metal centre; all values are typical for such types of interactions.

Vegard's Law[36] states that in solid solutions of isostructural compounds (i) the unit cell volume is proportional to the cube of the mean ionic radius and (ii) the unit cell dimensions (as well as mean bond lengths involving the metal atom) are linearly dependent on metal ion concentrations that are being substituted. We found that the unit cell dimensions (Table 1), unit cell volumes (Figure 6) and mean metal−ligand bond lengths (Figure 7) are indeed linearly dependent on the relative concentrations of the central cations, decreasing as Cd^{2+} is increasingly replaced by Ni^{2+}.

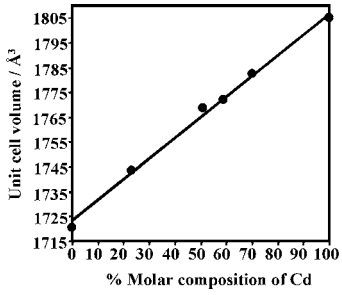

Figure 6. Unit cell volume vs. percentage molar composition of Cd

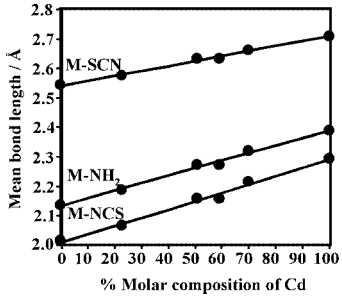

Figure 7. M−NCS bond length vs. percentage molar composition of Cd

We found parabolic behaviour instead of a linear correlation for the volume/ionic radii relationship (Figure 8). This has been observed in other situations before and is probably due the large difference in Cd and Ni ionic radii.[28]

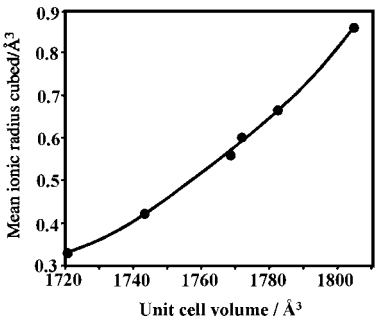

Figure 8. Cube of the mean ionic radii vs. unit cell volume

Infrared spectroscopy data substantiates a previous finding that NCS^- ligands acting as end-to-end bridging groups have CN stretching vibrations greater than 2100 cm^{-1}.[37] $\tilde{\nu}$(CN) for polymers **1**−**8** is 2124, 2125, 2123, 2124, 2122, 2121, 2118 and 2119 cm^{-1} respectively.

Elemental analysis results agree with the theoretical values. For **4**−**7**, calculated values were based on the relative amounts of cadmium and nickel determined by X-ray analysis, and were found to be in remarkably good agreement with the experimental values, indicating that the average composition of each batch is very close to that of the crystal chosen for X-ray analysis.

X-ray powder diffraction was used to confirm that all samples were uniform in that no structurally different compounds were present in the batch. In all instances, the calculated and experimental XRPD traces of product mixtures agreed; all peaks were present at the correct angular positions and with the correct relative intensities. For solid solutions **4**−**7** the calculated XRPD patterns are virtually identical, with only slight variations in some of the relative peak intensities. Therefore, this method was not sufficiently sensitive to differentiate between different ratios of the two metals present.

Thermal Analysis

Thermal analysis results are summarised in Table 4. For all compounds, the TG and DSC traces have the same profiles. TG traces consist of one-step mass losses due to the loss of two ABN ligands and a corresponding endotherm in the DSC trace. Experimental and calculated mass loss values are in good agreement (based on the composition determined by X-ray analysis).

We were able to determine the thermal stability of the polymers by measuring the onset temperature[38] (T_{on}) of decomposition due to the loss of two ABN ligands. The results show that thermal degradation of **1** and **2** occurs at the same onset temperature while polymer **3** is the most stable. For bimetallic polymers **4**−**7**, the results (Figure 9) indicate that their thermal stability is proportional to the amount of nickel present. This is to be expected as the higher percentage of cadmium causes the bonds (M−NCS, M−SCN and M−NH_2) around the metal centre to lengthen and, therefore, to weaken (Table 3). This result also accords with the rationalisation usually given for the relative positions of the main group cations in the Irving−Williams series.

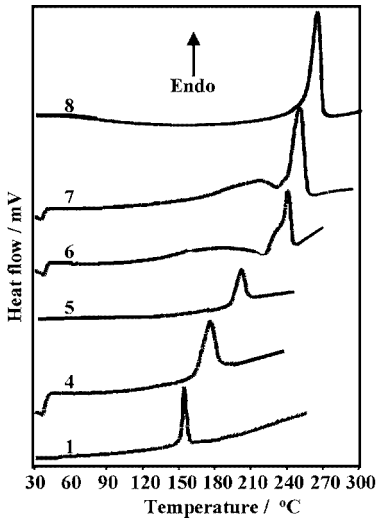

Figure 9. DSC results: migration of decomposition endotherm with changing Cd:Ni ratio

Conclusion

Aminobenzonitrile ligands can be used in the design and manipulation of new polymer architectures and their properties. In addition, the choice of metal ion influences the inclusion properties, thermal stability and structural features of the resultant coordination polymer. For example, at least one of the following is observed for the nickel and cadmium polymers (presented here and previously reported[22]): (i) the functionality through which ABNs are coordinated changes; (ii) both ABN and NCS^- ligands change their bonding environments from bidentate to monodentate coordination and vice versa; (iii) bridging and axial ligands are interchanged, (iv) inclusion properties are drastically affected and (v) thermal stability is influenced.

Comparison of all Ni and Cd polymer structures shows that, by changing the metal centre and/or adding a guest to the starting mixture, we can obtain three different polymer motifs (Scheme 1) that have different hydrogen-bonding capabilities, metal coordination environments and possible magnetic properties. [The nickel(II) coordination polymer, $Ni(NCS)_2(imidazole)_2$, which contains double thiocyanate bridges has been shown to exhibit long-range magnetic ordering.[39]]

Table 4. Thermal analysis data

	Polymer	**1**	**2**	**3**	**4**	**5**	**6**	**7**	**8**[22]
	M:L ratio	1:2	1:2	1:2	1:2	1:2	1:2	1:2	1:2
TG	Exp. mass loss (%)	50.1	50.4	50.9	52.1	53.7	53.1	56.2	57.3
	Calcd. mass loss (%)	50.8	50.8	50.8	52.7	53.3	53.9	55.8	57.5
DSC	T_{on} (°C)	147.9	148.0	182.9	160.0	190.3	239.5	244.2	246.6

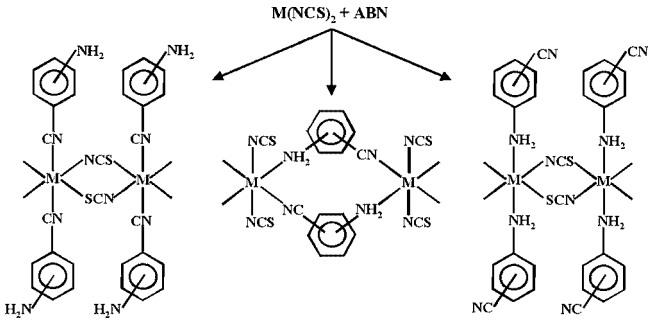

Scheme 1

By means of Vegard's Law,[36] it is possible to predict the composition of these solid solutions and, conversely, to ascertain their thermal stability from their composition.

We are currently attempting to develop a crystallisation methodology that would result in 2- and 3-dimensional ABN coordination polymers.

Experimental Section

Preparation of $[Cd(NCS)_2(3ABN)_2]_n$ (1), $[Cd(NCS)_2(2ABN)_2]_n$ (2) and $[Cd(NCS)_2(4ABN)_2]_n$ (3): The appropriate ABN isomer (0.047 g, 0.4 mmol) was dissolved in ethanol (0.5 mL) and added to ethanolic $Cd(NCS)_2$ solution (0.10 mmol·mL^{-1}, 1 mL). The resultant solution was then left to evaporate slowly, and gave colourless rectangular plate crystals within 24−72 h. Yield: **1**: 69%; **2**: 52%; **3**: 78%. **1:** $C_{16}H_{12}CdN_6S_2$; (464.84): calcd. C 41.34, H 2.60, N 18.08, S 13.80; found: C 41.34, H 2.41, N 18.06, S 13.73. **2**: $CdC_{16}H_{12}N_6S_2$ (464.84); for **2**: calcd. C 41.34, H 2.60, N 18.08 and S 13.80; found C 41.34, H 2.22, N 18.06, S 13.73. **3:** $CdC_{16}H_{12}N_6S_2$ (464.84):calcd. C 41.34, H 2.60, N 18.08, S 13.80 found C 41.35, H 2.52, N 18.10, S 13.77.

Preparation of Solid Solutions $[Cd_{1-x}Ni_x(NCS)_2(3ABN)_2]$ 4−7: 3ABN (0.35 g, 3.0 mmol) was dissolved in ethanol (3 mL) and added to solutions containing Ni^{II} and Cd^{II} in different ratios. To prepare the required metal ratios, ethanolic solutions of $Cd(NCS)_2$ (0.10 mmol·mL^{-1}) and $Ni(NCS)_2$ (0.20 mmol·mL^{-1}) were used. The solution of **4** contained $Ni(NCS)_2$ (1.25 mL) and $Cd(NCS)_2$ (7.50 mL) so that the Ni:Cd ratio was 25:75 while for **5** (Ni:Cd = 37:63) $Ni(NCS)_2$ (1.85 mL) and $Cd(NCS)_2$ (6.30 mL) were used. Compounds of **6** and **7** were prepared by adding $Ni(NCS)_2$ (2.50 and 3.75 mL) to $Cd(NCS)_2$ (5.0 and 2.5 mL) to give Ni:Cd ratios of 50:50 and 75:25 respectively. Crystals were obtained after 2−5 days for **4** and **5**, two weeks for **6** and approximately four weeks for **7**. The crystals varied from light green (**4**) to dark green (**7**) depending on the amount of nickel present. **4:** $C_{16}H_{12}Cd_{0.70}N_6Ni_{0.30}S_2$ (448.73): calcd. C 42.83, H 2.70, N 18.73, S 14.29; found C 42.72, H 2.58, N 18.69 and S 14.45. **5:** $C_{16}H_{12}Cd_{0.59}N_6Ni_{0.41}S_2$: (442.82): calcd. C 43.40, H 2.73, N 18.98, S 14.48; found C 43.21, H 2.52, N 19.05 and S 14.58. **6:** $C_{16}H_{12}Cd_{0.51}N_6Ni_{0.49}S_2$ (438.53): calcd. C 43.82, H 2.76, N 19.16, S 14.62; found C 43.94, H 2.48, N 19.24 and S 14.53. **7:** $C_{16}H_{12}Cd_{0.23}N_6Ni_{0.77}S_2$ (429.49): calcd. C 45.38, H 2.86, N 19.85, S 15.14; found C 45.62, H 2.52, N 19.58, S 15.26.

Thermal Analysis: Samples were crushed, blotted dry and sieved (Nybolt mesh) prior to analysis and then placed in open platinum pans for thermogravimetric (TG) experiments and in crimped but vented aluminium pans for differential scanning calorimetry (DSC). TG and DSC were carried out on a Perkin−Elmer PC7-Series system over the range 30−500 °C, at a heating rate of 20 °C min^{-1}, with a purge of dry nitrogen (30 mL·min^{-1}). Thermal analysis experiments depend on sample preparation, instrument geometry and heating rates. Particle size in particular can have a significant influence on the onset temperature of the thermal events[40]. Therefore, care was taken to prepare all samples in the same, reproducible manner. Each sample was sieved through a Nybolt mesh with a pore size of 17−80 μm.

Structure Determination: Cell dimensions were obtained from the intensity data measurements on a Nonius−Kappa CCD diffractometer using graphite-monochromated Mo-K_α radiation (λ = 0.71069 Å). The strategy for data collection was evaluated using the COLLECT[41] software. For all five structures, data were collected at 173(2) K using standard φ-scan and ω-scan techniques. All sets of data were scaled and reduced using DENZO-SMN.[42] Structures were solved by direct methods using SHELX-86[43] and refined by full-matrix least-squares with the program SHELX-97,[44] refining on F^2. The program X-Seed[45] was used as a graphical interface for structure solution and refinement using SHELX. No absorption corrections were necessary. Important crystal and experimental data for all five structures are given in Table 1.

Elemental Analysis: Elemental analyses to determine the percentages of C, H, N, and S were made on a Carlo−Erba 1106 Elemental Analyser. For each sample, the analysis was carried out in duplicate.

Infrared Spectroscopy: IR spectra were recorded using a Perkin−Elmer 983 IR spectrophotometer and NaCl plates. Samples were run as Nujol mulls over the range 4000−400 cm^{-1} and analysed for the mode of thiocyanate coordination.

Electron Microscopy: Single crystals were mounted using carbon glue and coated with a layer of pure carbon by vacuum evaporation. The analysis was performed on a Leo S440, fully analytical electron microscope with a KEVEX energy dispersive spectrometer. Data were collected at 30 kV with a beam current of 100 pA at a distance of 20 mm, tilt angle of 0° and a take-off angle of 35°. The results were analysed using the KEVEX Sigma Quasar Pro program.

X-ray Powder Diffraction (XRPD): X-ray powder diffraction patterns were measured using a Philips PW1050/25 goniometer with nickel-filtered Cu-K_α radiation. Samples were packed in aluminium sample holders and a step size of 0.1° at a scan rate of 1 s per step in the 2θ range 6−40° was employed for analysis. Calculated XRPD traces were generated for comparison purposes from the crystal structure results using the program LAZYPULVERIX.[46] CCDC-233623 to -233629 contain the supplementary crystallographic data for this paper. These data can be obtained free of charge at www.ccdc.cam.ac.uk/conts/retrieving.html [or from the Cambridge Crystallographic Data Centre, 12 Union Road, Cambridge CB2 1EZ, UK; Fax: (internat.) +44-1223-336-033; E-mail: deposit@ccdc.cam.ac.uk].

Acknowledgments

We thank the Claude Harris Leon Foundation for financial support.

[1] D. K. Chand, K. Biradha, M. Fujita, S. Sakamoto, K. Yamaguchi, *Chem. Commun.* **2002**, 2486.

[2] B. Moulton, M. J. Zaworotko, *Chem. Rev.* **2001**, *101*, 1629.
[3] H. Hou, Y. Fan, L. Zhang, C. Du, Y. Zhu, *Inorg. Chem. Commun.* **2001**, *4*, 168.
[4] G. F. Swiegers, T. J. Malefetse, *Chem. Rev.* **2000**, *100*, 3483.
[5] M. J. Zaworotko, *Angew. Chem. Int. Ed.* **2000**, *39*, 3053.
[6] K. Biradha, Y. Hongo, M. Fujita, *Angew. Chem. Int. Ed.* **2000**, *39*, 3843.
[7] B. Moulton, M. J. Zaworotko, *Curr. Opin. Solid State Mater. Sci.* **2002**, *6*, 117.
[8] J. D. Hartgerink, E. R. Zubarev, S. I. Stupp, *Curr. Opin. Solid State Mater. Sci.* **2001**, *5*, 355.
[9] S. R. Batten, *Curr. Opin. Solid State Mater. Sci.* **2001**, *5*, 107.
[10] L. Ma, O. R. Evans, B. M. Foxman, W. Lin, *Inorg. Chem.* **1999**, *38*, 5837.
[11] N. Singh, R. K. Sinha, *Inorg. Chem. Commun.* **2003**, *6*, 97.
[12] N. Singh, R. K. Sinha, *Inorg. Chem. Commun.* **2002**, *5*, 255.
[13] B. Żurowska, J. Mroziński, M. Julve, F. Lloret, A. Maslojeva, W. Sawska-Dobrowolska, *Inorg. Chem.* **2002**, *41*, 1771.
[14] M. A. Lawandy, X. Huang, R.-J. Wang, J. Li, J. Y. Lu, *Inorg. Chem.* **1999**, *38*, 5410.
[15] J. Y. Lu, C. Norman, K. Abboud, A. Ison, *Inorg. Chem. Commun.* **2001**, *4*, 459.
[16] M. Fujita, J. W. Kwon, S. Washizu, *J. Am. Chem. Soc.* **1994**, *116*, 1151.
[17] B. F. Abrahams, B. F. Hoskins, D. M. Michail, R. Robson, *Nature* **1994**, *369*, 727.
[18] S. Subramanian, M. J. Zaworotko, *Angew. Chem. Int. Ed. Engl.* **1995**, *34*, 2127.
[19] J. L. Atwood, L. J. Barbour, A. Jerga, *Science* **2002**, *296*, 2367.
[20] W. Lin, Z. Wang, L. Ma, *J. Am. Chem. Soc.* **1999**, *121*, 11249.
[21] H. Hou, Y. Wei, Y. Fan, C. Du, Y. Zhu, Y. Song, Y. Niu, X. Xin, *Inorg. Chim. Acta* **2001**, *319*, 212.
[22] D. Vujovic, H. G. Raubenheimer, L. R. Nassimbeni, *Dalton Trans.* **2003**, 631.
[23] Y.-B. Dong, M. D. Smith, H.-C. zur Loye, *Inorg. Chem.* **2000**, *39*, 1943.
[24] N. Singh, S. Gupta, *Inorg. Chem. Commun.* **2000**, *3*, 446.
[25] D. M. Ciurtin, M. D. Smith, H.-C. zur Loye, *Inorg. Chim. Acta* **2001**, *324*, 46.
[26] S. Nagata, *J. Phys. Soc., Jpn.* **1974**, *37*, 645.
[27] Y. Mathey, C. Mazieres, *Bull. Soc. Chim. France* **1973**, *11*, 2918.
[28] T. Miyoshi, T. Iwamoto, Y. Sasaki, *Inorg. Chim. Acta* **1973**, 97.
[29] T. Miyoshi, T. Iwamoto, Y. Sasaki, *Inorg. Chim. Acta* **1968**, 329.
[30] H. Zhang, X. Wang, K. Zhang, B. K. Teo, *Coord. Chem. Rev.* **1999**, 157.
[31] W. Chen, F. Liu, X. You, *Bull. Chem. Soc., Jpn.* **2002**, *75*, 1559.
[32] M. A. S. Goher, F. A. Mautner, M. A. M. Abu-Youssef, A. K. Hafez, A. M.-A. Badr, C. Gspan, *Polyhedron* **2003**, *22*, 3137.
[33] S. G. Bott, B. D. Fahlman, M. L. Pierson, A. R. Barron, *J. Chem. Soc., Dalton Trans.* **2001**, 2148.
[34] B. K. Vainshtein, V. M. Fridkin, V. L. Indenbom, *Modern Crystallography 2, Structure of Crystals*, Springer-Verlag, Berlin, **1995**, ch. 1, pp. 113.
[35] R. Shannon, *Acta Crystallogr., Sect. A* **1976**, *32*, 751.
[36] R. M. Hazen, L. W. Finger, in *Comparative Crystal Chemistry: Temperature, Pressure, Composition and the variation of Crystal Structure*, Wiley-VCH, Weinheim, **1982**, ch. 8, pp. 168.
[37] K. Nakamoto, *Infrared and Raman Spectra of Inorganic and Coordination Compounds*, Wiley, New York, **1978**, ch. 3, pp. 270.
[38] M. R. Caira, L. R. Nassimbeni, in *Comprehensive Supramolecular Chemistry* (Eds. J. L. Atwood, J. E. D. Davies, D. D. MacNicol, F. Vögtle), Elsevier Science, Oxford, **1996**, vol. 6, ch. 25, pp. 825.
[39] B. Żurowska, J. Mroziński, M. Julve, F. Lloret, A. Maslojeva, W. Sawska-Dobrowolska, *Inorg. Chem.* **2002**, *41*, 1771.
[40] M. E. Brown, *Introduction to Thermal Analysis*, Academic Press, Boston, **1990**, ch. 1, pp. 15.
[41] COLLECT, data collection software, Nonius, **1998**.
[42] Z. Otwinowski, W. Minor, in *Methods in Enzymology*, vol. 276: *Macromolecular Crystallography*, part A (Eds.: C. W. Carter Jr., R. M. Sweet), Academic Press, **1997**, pp. 307.
[43] G. M. Sheldrick, SHELX-86, in *Crystallographic Computing 3* (Eds.: G. M. Sheldrick, C. Kruger, R. Goddard), Oxford University Press, Oxford, **1985**, pp. 75.
[44] G. M. Sheldrick, T. R. Schneider, in *SHELXL: High-Resolution Refinement, Methods in Enzymology*, vol. 277 (Macromolecular Crystallography, Part B (Eds.: C. W. Carter, R. M. Sweet), **1997**, pp. 319.
[45] L. J. Barbour, *J. Supramol. Chem.* **2001**, *1*, 189.
[46] K. Yvon, W. Jeitschko, E. Parthe, *J. Appl. Cryst.* **1977**, *10*, 73.

Received October 29, 2003
Early View Article
Published Online May 5, 2004

